

# Probing the hidden gauge symmetry breaking through the phase transition gravitational waves

Fa Peng Huang\* and Xinmin Zhang

*Theoretical Physics Division, Institute of High Energy Physics,  
Chinese Academy of Sciences, P.O.Box 918-4, Beijing 100049, P.R.China*

Motivated by the discovery of gravitational waves (GWs) at aLIGO and no evidence of new physics at current LHC, we discuss that a generic classes of extended new physics models with hidden gauge group could undergo one or several times first-order phase transitions associated with the gauge group symmetry breaking during the evolution of the universe, which might produce detectable phase transition GWs signals at future GWs experiments, such as eLISA and BBO.

PACS numbers: 04.30.-w, 11.15.Ex, 12.60.-i

## I. INTRODUCTION

The observation of gravitational waves (GWs) by Advanced Laser Interferometer Gravitational Wave Observatory (aLIGO) [1] has initiated a new era of exploring the cosmology, the nature of gravity as well as the fundamental particle physics by the GWs detectors [2–8]. Especially, due to the limitation of the colliders' energy, GWs detectors can be used as new techniques to probe the symmetry breaking patterns or phase transition history for a large class of new physics models with hidden gauge group extensions of the standard model (SM), which are motivated by the mysterious experimental results in our understanding of particle cosmology (such as the dark matter problem or the puzzling observed baryon asymmetry of the universe), and the absence of new physics signals at current collider experiments. The increasingly attractive new physics models with hidden gauge group extensions of the SM have many new particles without leaving any observable imprints at current particle colliders. However, the GWs experiments may provide a possible approach to test their existence. For example, to explain the baryon asymmetry of the universe via electroweak baryogenesis by the hidden gauge group extended model, a strong first-order phase transition is needed to realize the departure from thermal equilibrium [9–11]. And during the first-order phase transition, the detectable GWs will be produced through three mechanisms: collisions of expanding bubbles, sound waves, and magnetohydrodynamic turbulence of bubbles in the hot plasma [12–19]. Phase transitions in particle physics and cosmology are usually associated with the symmetry breaking, i.e. where the universe transits from a symmetric phase to a symmetry broken phase when the temperature drops below the corresponding critical temperature.

For the first time, we have a chance to explore the hidden gauge symmetry breaking through phase transition GWs signals after the discovery of the GWs by aLIGO, which is particularly exciting. In this paper, we study the possibility to explore the hidden gauge symmetry breaking patterns by the phase transition GWs signals. In particular, we will focalize our analysis to GWs detection of the non-Abelian gauge group extended models, where the symmetry breaking at each energy scale may associate with a first-order phase transition, as shown in Fig.1. The hidden group  $G_{\text{Hidden}}$ , which can spontaneously breaks into the SM gauge group  $G_{\text{SM}} : SU(3)_c \otimes SU(2)_L \otimes U(1)_X$ . During the hidden gauge symmetry breaking, a strong first-order phase transition can take place, which will produce detectable phase transition GWs. For example, the hidden gauge group  $G_{\text{Hidden}}$  can be the non-Abelian group  $SU(3)_c \otimes SU(3)_L \otimes U(1)_Y$ , and the model is called 3-3-1 model [20, 21]. We show that many versions of the 3-3-1 model can produce at least one time strong first-order phase transitions at the energy of several TeV in some parameter spaces, which can produce detectable GWs spectrum by Evolved Laser Interferometer Space Antenna (eLISA) [22], Big Bang Observer (BBO) [23]. In general, there can exist several times spontaneous symmetry breaking, which may also accompany several times first-order phase transition during the evolution of the universe as shown in Fig.1. If the energy scale of the symmetry breaking and the associated first-order phase transition range from  $10^7$  to  $10^8$  GeV triggered by the hidden sector, the phase transition GWs spectrum may be within the sensitivity of future aLIGO. Other attractive examples of GWs detection of the non-Abelian gauge group extended models are also discussed, such as the first-order dark QCD phase transition GWs in the relaxion mechanism [24], which may be tested by pulsar time array (PTA) at the Square Kilometre Array (SKA) [25] or the Five-hundred-meter Aperture Spherical Telescope (FAST) [26] in China. The other one is the Naturalness mechanism [27], which may also produce observable phase transition GWs signals at the GWs

---

\*Electronic address: huangfp@ihep.ac.cn

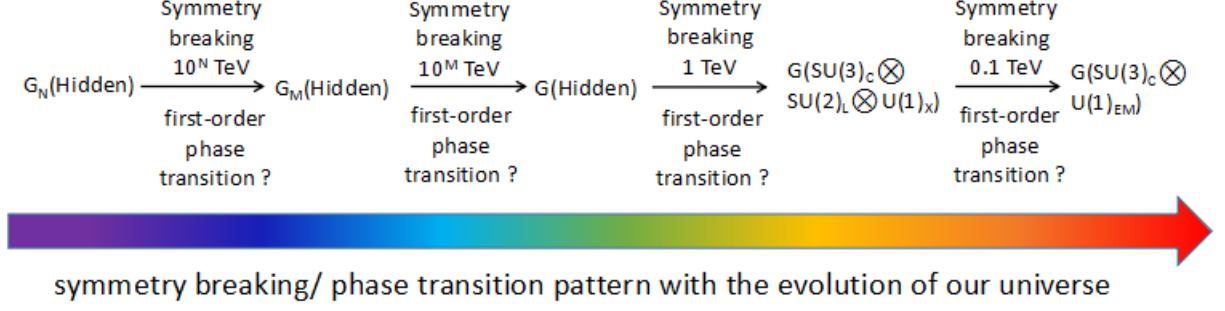


FIG. 1: Symmetry breaking (phase transition) patterns for the non-Abelian gauge group extended models with the evolution of our universe, where the first-order phase transitions may happen.

detector.

This paper is organized as follows: In Section II, we schematically discuss the GWs detection of the hidden gauge group symmetry breaking and show how to calculate the phase transition GWs during the first-order phase transition. In Section III, we will study the phase transition GWs spectra in some concrete hidden gauge group extended models. In Section IV, we show our final discussions and conclusions.

## II. FIRST-ORDER PHASE TRANSITION GWS SPECTRUM

In a large class of new physics models with extended non-Abelian hidden gauge group, one or several times cosmological phase transitions can occur during each step's hidden gauge symmetry breaking. In general, we can have the gauge symmetry breaking patterns with the extended hidden gauge group at each scales with the evolution of the universe as shown in Fig. 1. For example, the hidden symmetry breaking pattern may be the following:

$$G(\text{Hidden } N) \cdots \rightarrow G(\text{Hidden } 1) \rightarrow G(SU(3)_C \otimes SU(3)_L \otimes U(1)_Y) \rightarrow G(SU(3)_C \otimes SU(2)_L \otimes U(1)_X) \rightarrow G(SU(3)_C \otimes U(1)_{EM}).$$

With the evolution of our universe, symmetry breaking will happen at corresponding energy scale, where the strong first-order phase transition may take place. Detailed models are given in Section III.

Along with the symmetry breaking from a 'false' vacuum to a 'true' vacuum, strong first-order phase transition occurs if there exists a sufficient potential barrier between them. This process can produce an observable stochastic GWs signals, which can be detected in some GWs detectors, such as aLIGO, eLISA, BBO, SKA, FAST and so on. Their sensitivity range for some critical temperatures depends on the energy scale of the first-order phase transition for different hidden gauge group extended models, as shown in section III.

To discuss the GWs spectrum from the first-order phase transition, it is necessary to begin with the one-loop finite temperature effective potential:

$$V_{\text{eff}}(\Phi, T) = V_{\text{tree}}(\Phi) + V_{\text{CW}}(\Phi) + V_{\text{thermal}}(\Phi, T) + V_{\text{daisy}}(\Phi, T), \quad (1)$$

where  $\Phi$  represents the order parameter of the phase transition (a real scalar field),  $V_{\text{CW}}(\Phi)$  is the one-loop Coleman-Weinberg potential at  $T = 0$ , and  $V_{\text{thermal}}(\Phi, T) + V_{\text{daisy}}(\Phi, T)$  is the thermal contribution including the daisy resummation [28].

During each step of symmetry breaking in the hidden gauge group extended models, strong first-order phase transition may occur. During the first-order phase transition, bubbles are nucleated via quantum tunneling or thermally fluctuating the potential barrier. The bubble nucleation rate per unit volume  $\Gamma$  is given by  $\Gamma = \Gamma_0(T)e^{-S_E(T)}$  with  $\Gamma_0(T) \propto T^4$  [29], where  $S_E(T)$  is the Euclidean action [30, 31] defined as

$$S_E(T) = \int d\tau d^3x \left[ \frac{1}{2} \left( \frac{d\Phi}{d\tau} \right)^2 + \frac{1}{2} (\nabla\Phi)^2 + V_{\text{eff}}(\Phi, T) \right]. \quad (2)$$

Here,  $S_E(T) \simeq S_3(T)/T$ , and  $\Gamma = \Gamma_0 e^{-S_3/T}$  [29] where

$$S_3(T) = \int d^3x \left[ \frac{1}{2} (\nabla\Phi)^2 + V_{\text{eff}}(\Phi, T) \right]. \quad (3)$$

From the above equations, in order to obtain the bubble nucleation rate, the profile of the scalar field  $\Phi$  during the bubble nucleation needs to be calculated by solving the following bounce equation:

$$\frac{d^2\Phi}{dr^2} + \frac{2}{r} \frac{d\Phi}{dr} - \frac{\partial V_{\text{eff}}(\Phi, T)}{\partial \Phi} = 0, \quad (4)$$

with the boundary conditions

$$\frac{d\Phi}{dr}(r=0) = 0, \quad (5)$$

$$\Phi(r=\infty) = \Phi_{\text{false}}. \quad (6)$$

The bounce equation can be solved numerically using the overshoot/undershoot method. The first-order phase transition terminates when nucleation probability of one bubble per horizon volume is of  $\mathcal{O}(1)$ , i.e.,  $\Gamma(T_*) \simeq H_*^4$ . That is to say, it should satisfy

$$S_3(T_*)/T_* = 4 \ln(T_*/100\text{GeV}) + 137. \quad (7)$$

It is known that there exist three major sources for producing GWs during the first-order phase transition, which are collisions of the vacuum bubbles [15], sound waves [16] and turbulence [17, 18] in the plasma after collisions, respectively.

The most well-known source is the bubbles collisions, and the first-order phase transition GWs spectrum depends on four parameters. The first one is the ratio  $\alpha$  of the vacuum energy density released in the phase transition to that of the thermal bath, defined as

$$\alpha \equiv \frac{\epsilon(T_*)}{\rho_{\text{rad}}(T_*)}, \quad (8)$$

where  $*$  specifies that the quantity is evaluated at the time  $T_*$  determined by Eq.(7). Note that, the false vacuum energy density  $\epsilon(T_*) = [T \frac{dV_{\text{eff}}^{\text{min}}}{dT} - V_{\text{eff}}^{\text{min}}(T)]|_{T=T_*}$  is the latent heat density, and the plasma thermal energy density  $\rho_{\text{rad}}(T_*)$  is equal to  $\frac{\pi^2}{30} g_*(T) T^4$ . Here,  $V_{\text{eff}}^{\text{min}}(T)$  is the temperature-dependent true minimum of the effective potential of the scalar field, which is responsible for the phase transition. The parameter  $\alpha$  measures the strength of the phase transition GWs, namely, larger values for  $\alpha$  correspond to stronger first-order phase transition GWs.

The second one is the time duration of the phase transition  $\beta^{-1}$ , where one has  $\beta \equiv -\frac{dS_E}{dt}|_{t=t_*} \simeq \frac{1}{\Gamma} \frac{d\Gamma}{dt}|_{t=t_*}$ . In other words,  $\beta^{-1}$  corresponds to the typical time scale of the phase transition. Since  $\beta = \dot{\Gamma}/\Gamma$  during the phase transition from its definition, one has

$$\frac{\beta}{H_*} = T \left. \frac{d(S_3/T)}{dT} \right|_{T=T_*}. \quad (9)$$

The third one is the efficiency factor  $\lambda$ , which characterizes the fraction of the energy density converted into the motion of the colliding bubble walls and the last one is the bubble wall velocity  $v_b$ . The energy released into the GWs of peak frequency is then given by [32]:

$$\frac{\rho_{\text{GW}}}{\rho_{\text{tot}}} \sim \theta \left( \frac{H_*}{\beta} \right)^2 \lambda^2 \frac{\alpha^2}{(1+\alpha)^2} v_b^3. \quad (10)$$

The second and third sources are the GWs from the matter fluid effects, which can further contribute to the total energy released in gravitational radiation during the phase transition. Here, we just use the formulae given in [33]. One source is from the sound waves in the fluid, where a certain fraction  $\lambda_v$  of the bubble wall energy (after the collision) is converted into motion of the fluid (and is only later dissipated) with the following contribution

$$\frac{\rho_{\text{GW},sw}}{\rho_{\text{tot}}} \sim \theta_{sw} \left( \frac{H_*}{\beta} \right) \lambda_v^2 \left( \frac{\alpha^2}{(1+\alpha)^2} \right). \quad (11)$$

The other one is from turbulence in the fluid, where a certain fraction  $\lambda_{tu}$  of the walls energy is converted into turbulence, with the contribution

$$\frac{\rho_{\text{GW},turb}}{\rho_{\text{tot}}} \sim \theta_{tu} \left( \frac{H_*}{\beta} \right) \lambda_{tu}^{3/2} \left( \frac{\alpha^{3/2}}{(1+\alpha)^{3/2}} \right). \quad (12)$$

It is worth noticing that these two contributions from the matter fluid effects depend on  $H_*/\beta$  linearly, and they are not fully understood. In some cases, these two effects may be larger than the one from bubble collisions.

The peak frequency produced by bubble wall collisions at  $T_*$  during the first-order phase transition is given by [36, 37]:  $f_{\text{co}}^* = 0.62\beta/(1.8 - 0.1v_b + v_b^2)$ . Considering the adiabatic expansion of our universe from the early universe to the present universe, the ratio of scale factors at the time of first-order phase transition and today can be written as

$$\frac{a_*}{a_0} = 1.65 \times 10^{-5} \text{Hz} \times \frac{1}{H_*} \left( \frac{T_*}{100 \text{GeV}} \right) \left( \frac{g_*^t}{100} \right)^{1/6}, \quad (13)$$

where  $g_*^t$  is the effective degrees of freedom at  $T_*$ . Thus, the peak frequency today is  $f_{\text{co}} = f_{\text{co}}^* a_*/a_0$ , and the corresponding GWs intensity is given by [36]

$$\begin{aligned} \Omega_{\text{co}}(f)h^2 &\simeq 1.67 \times 10^{-5} \left( \frac{H_*}{\beta} \right)^2 \left( \frac{\lambda\alpha}{1+\alpha} \right)^2 \left( \frac{100}{g_*^t} \right)^{\frac{1}{3}} \\ &\times \left( \frac{0.11v_b^3}{0.42 + v_b^3} \right) \left[ \frac{3.8(f/f_{\text{co}})^{2.8}}{1 + 2.8(f/f_{\text{co}})^{3.8}} \right]. \end{aligned}$$

The peak frequency of the GWs signals due to the sound wave effects is about  $f_{\text{sw}}^* = 2\beta/(\sqrt{3}v_b)$  [16, 33], and similarly its current value is  $f_{\text{sw}} = f_{\text{sw}}^* a_*/a_0$ . In this case, the GWs intensity is expressed as [16, 33]

$$\begin{aligned} \Omega_{\text{sw}}(f)h^2 &\simeq 2.65 \times 10^{-6} \left( \frac{H_*}{\beta} \right) \left( \frac{\lambda_v\alpha}{1+\alpha} \right)^2 \left( \frac{100}{g_*^t} \right)^{\frac{1}{3}} v_b \\ &\times \left[ \frac{7(f/f_{\text{sw}})^{6/7}}{4 + 3(f/f_{\text{sw}})^2} \right]^{7/2}, \end{aligned}$$

in which  $\lambda_v \simeq \alpha(0.73 + 0.083\sqrt{\alpha} + \alpha)^{-1}$  for relativistic bubbles [34].

The GWs signals produced from the turbulence in the plasma have the peak frequency at about  $f_{\text{tu}}^* = 1.75\beta/v_b$  [33], which determines the current value as  $f_{\text{tu}} = f_{\text{tu}}^* a_*/a_0$  after considering the red shift. The phase transition GWs intensity from turbulence is formulated by [18, 35]

$$\begin{aligned} \Omega_{\text{tu}}(f)h^2 &\simeq 3.35 \times 10^{-4} \left( \frac{H_*}{\beta} \right) \left( \frac{\lambda_{\text{tu}}\alpha}{1+\alpha} \right)^{3/2} \left( \frac{100}{g_*^t} \right)^{\frac{1}{3}} v_b \\ &\times \frac{(f/f_{\text{tu}})^3}{(1 + f/f_{\text{tu}})^{11/3} (1 + 8\pi f a_0 / (a_* H_*))}. \end{aligned}$$

The final phase transition spectrum consists of the three contributions above.

### III. PHASE TRANSITION GWS FROM NON-ABELIAN GAUGE GROUP EXTENDED MODELS

In this section, we discuss the phase transition GWs in some non-Abelian gauge group extended models in details, where one or several times symmetry breaking and first-order phase transition may occur with the evolution of our universe at certain critical temperature. Firstly, the GWs spectra in the hidden gauge group extended models based on the  $SU(3)_c \otimes SU(3)_L \otimes U(1)_Y$  gauge symmetry, commonly known as the 3-3-1 model [20, 21] are investigated. The 3-3-1 models can explain the electric charge quantization and three generations of fermions [20, 21]. The collider phenomenology of the 3-3-1 models has been extensively studied, such as the recent Ref. [38] and references therein, and the phase transitions in some versions of 3-3-1 models have been studied by Refs. [39–41]. Here, we try to explore the possible phase transition patterns associated with the symmetry breaking  $SU(3)_L \otimes U(1)_Y \rightarrow SU(2)_L \otimes U(1)_X \rightarrow U(1)_{\text{EM}}$  using the phase transition GWs in some versions of the 3-3-1 models, where the scalar fields are accommodated in a certain representation of the  $SU(3)_L$  gauge group in each version.

In the following, we will show three versions of 3-3-1 models (the minimal, the economical and the reduced minimal 3-3-1 models, respectively) [39–41], where very strong first-order phase transitions can take place at the TeV scale [39–41] and produce detectable phase transition GWs by eLISA and BBO. For simplicity, we limit our discussion of the first-order phase transition to the thermal barrier case, where the potential barrier in the finite temperature effective potential origins from thermal loop effects. In this type of thermal barrier case, the bosonic fields contribute to the thermal effective potential of the form  $V_{\text{eff}} \ni (-T/12\pi)(m_{\text{boson}}^2(X, T))^{3/2}$  in the limit of high-temperature expansion.

To begin with the concrete prediction of the GWs in the following examples, we first discuss the general effective potential near the symmetry breaking and phase transition temperature, which can be approximated by

$$V_{\text{eff}}(X, T) \approx \frac{1}{2} (-\mu^2 + cT^2) X^2 - \frac{eT}{12\pi} (X^2)^{3/2} + \frac{\lambda}{4} X^4. \quad (14)$$

Here,  $X$  represents the field of the order parameter for the phase transition. For the electroweak phase transition in the SM,  $X$  field is just the Higgs field. The parameter  $e$  quantify the interactions between  $X$  field and the light bosons, and can be schematically written as  $e \sim \sum_{\text{light bosonic fields}} (\text{degrees of freedom}) \times (\text{coupling to } X)^{3/2}$ . And, the parameters  $c$  depends on interaction between  $X$  and light bosons and fermions. For the heavy fields whose masses are much larger than the critical temperature, their contribution can be omitted from Boltzmann suppression. This can help to simplify our discussions when the models have many new fields at different energy scales. Thus, in this case of qualitative analysis, the wash out parameter can be obtained as

$$\frac{\langle X \rangle(T_c)}{T_c} \approx \frac{e}{6\pi\lambda}, \quad (15)$$

where the angle bracket means the vacuum expectation value (VEV) of the field  $X$  at the critical temperature  $T_c$ . From the above qualitative analysis, we know that introducing new light bosonic fields (compared to the corresponding critical temperature) helps to produce or enhance the first-order phase transition. The 3-3-1 models just introduce enough bosonic fields to produce detectable phase transition GWs.

#### A. Phase transition GWs spectrum in the economical 3-3-1 model and the reduced minimal 3-3-1 model

We consider the first-order phase transition GWs spectrum in the so-called economical 3-3-1 model [40]. In this version of 3-3-1 model, one chooses the simplest  $SU(3)_L$  representations for the scalar fields with spontaneously symmetry breaking, namely, two complex scalar triplets with different hypercharge are needed as follows

$$\chi = (\chi_1^0, \chi_2^-, \chi_3^0)^T \sim \left(3, -\frac{1}{3}\right), \quad (16)$$

$$\phi = (\phi_1^+, \phi_2^0, \phi_3^+)^T \sim \left(3, \frac{2}{3}\right). \quad (17)$$

The scalar potential is written as

$$V(\chi, \phi) = \mu_1^2 \chi^\dagger \chi + \lambda_1 (\chi^\dagger \chi)^2 + \mu_2^2 \phi^\dagger \phi + \lambda_2 (\phi^\dagger \phi)^2 + \lambda_3 (\chi^\dagger \chi)(\phi^\dagger \phi) + \lambda_4 (\chi^\dagger \phi)(\phi^\dagger \chi). \quad (18)$$

The  $SU(3)_L \otimes U(1)_Y$  gauge group is broken spontaneously via two steps. In the first step, the symmetry breaking  $SU(3)_L \otimes U(1)_Y \rightarrow SU(2)_L \otimes U(1)_X$  happens when the scalar triplet  $\chi$  acquired with the VEV given by

$$\langle \chi \rangle = \frac{1}{\sqrt{2}} (u, 0, \omega)^T. \quad (19)$$

In the last step, to break into the SM  $U(1)_{\text{EM}}$  gauge group  $SU(2)_L \otimes U(1)_X \rightarrow U(1)_{\text{EM}}$ , another scalar triplet  $\phi$  is needed to acquire the VEV as follows

$$\langle \phi \rangle = \frac{1}{\sqrt{2}} (0, v, 0)^T. \quad (20)$$

In this version of 3-3-1 model, there exist two neutral scalars<sup>1</sup>, one is the SM Higgs boson  $h$ , the other is the heavy scalar  $H_1$ . In this paper, the packet ‘CosmoTransitions’ [42] is used to numerically calculate the first-order phase transition. During the first symmetry breaking  $SU(3)_L \otimes U(1)_Y \rightarrow SU(2)_L \otimes U(1)_X$ , the order parameter field for the

---

<sup>1</sup> Here, we do not present the details of the other interactions and the whole particle spectra. Details on the parameter space discussions of phase transition in this model can see Ref. [40].

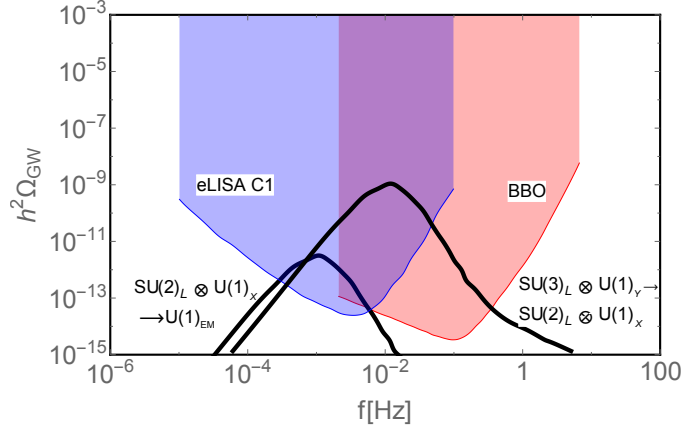


FIG. 2: The phase transition GWs spectra  $h^2\Omega_{\text{GW}}$  for the economical 3-3-1 model. The colored regions correspond to the expected sensitivities of GWs interferometers eLISA and BBO, respectively. The black line depicts the GWs spectra for the two times first-order phase transition during  $SU(3)_L \otimes U(1)_Y \Rightarrow SU(2)_L \otimes U(1)_X$  at the TeV (right line) scale and  $SU(2)_L \otimes U(1)_X \Rightarrow U(1)_{\text{EM}}$  at the electroweak scale (left line), respectively.

phase transition is approximately the  $H_1$  scalar field, namely, the  $X = H_1$  field if it is compared to Eq.(14). Strong first-order phase transition at the energy scale of several TeV can be induced by the new bosons and exotic quarks in this version of 3-3-1 model if the mass of these new particle are from  $10^2$  GeV to several TeV. During the last symmetry breaking  $SU(2)_L \otimes U(1)_X \rightarrow U(1)_{\text{EM}}$ , the order parameter field for the phase transition is approximately the Higgs field, namely, the  $X = h$  field if it is compared to Eq.(14). First-order phase transition at the electroweak scale can be triggered by the new bosons and it is rather weak than the first step. For the set of benchmark points<sup>2</sup> of  $m_{H_1} = 1.4$  TeV,  $m_{H_2^\pm} = 3.2$  TeV, using the methods and formulae in the above Section II and the package ‘CosmoTransitions’ [42], these two times first-order phase transition will produce two copies GWs spectra with different characteristic peak frequency and amplitude, as shown in Fig. 2. It shows that the phase transition GWs can be used to explore the symmetry breaking and phase transition patterns by eLISA and BBO.

The GWs spectra of the reduced minimal 3-3-1 model is similar to the one of the economical 3-3-1 model since their symmetry breaking and phase transition patterns are similar to the economical model. The reduced minimal 3-3-1 model is mainly composed by neutral scalars  $h$ ,  $H_1$ , doubly charged scalar  $h^{++}$ , two SM like bosons  $Z_1$ ,  $W^\pm$ , the new heavy neutral boson  $Z_2$ , the singly and doubly charged boson  $U^{\pm\pm}$  and  $U^{\pm}$ . These new particles and exotic quarks can be triggers for the first-order phase transition [41]. Taking use of the methods and formulae in Sec.II and the package ‘CosmoTransitions’ [42], for the set of benchmark points  $m_{H_1} = 1.3$  TeV,  $m_{h^{++}} = 3.3$  TeV, two copies GWs spectra during two times first-order phase transition will be produced, as shown in Fig. 3, which can also be detected by eLISA and BBO.

### B. Phase transition GWs spectrum in the minimal 3-3-1 model

The minimal 3-3-1 model [39] corresponds to the parameter  $\beta = -\sqrt{3}$  [39] in the definition of the electric charge operator. The gauge bosons, associated with the gauge symmetry  $SU(3)_L \otimes U(1)_Y$  of the model, consist of an octet  $W_\mu^i$  ( $i = 1, \dots, 8$ ) and a singlet  $B_\mu$ . In this version of 3-3-1 model, three  $SU(3)_L$  triplets scalars are needed to break the symmetry and generate the mass of gauge bosons and exotic quarks as the following

$$\begin{aligned}\eta &= (\eta^0 \ \eta_1^- \ \eta_2^+)^T, \\ \rho &= (\rho^+ \ \rho^0 \ \rho^{++})^T, \\ \chi &= (\chi^- \ \chi^{--} \ \chi^0)^T.\end{aligned}\tag{21}$$

<sup>2</sup> We show only one set of benchmark points to avoid confusion between the GWs spectra from two times first-order phase transition and the GWs spectra for one time first-order phase transition with two sets of benchmark points.

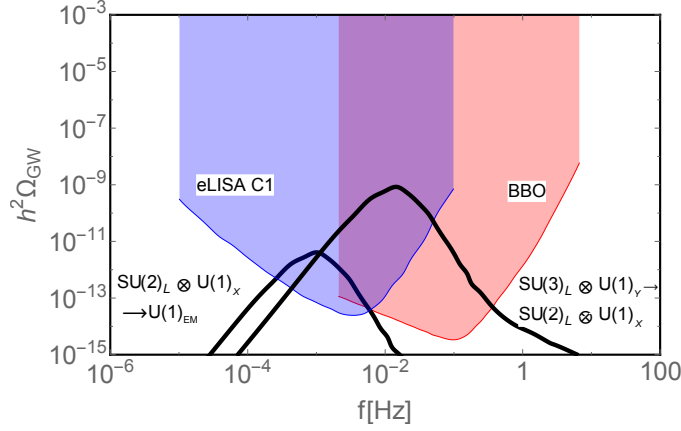


FIG. 3: The GWs spectra  $h^2\Omega_{\text{GW}}$  for the reduced minimal 3-3-1 model. The colored regions correspond to the expected sensitivities of GW interferometers eLISA and BBO, respectively. The black line depicts the GWs spectrum for the two times first-order phase transition during  $SU(3)_L \otimes U(1)_Y \Rightarrow SU(2)_L \otimes U(1)_X$  at the TeV scale (right line) and  $SU(2)_L \otimes U(1)_X \Rightarrow U(1)_{\text{EM}}$  at the electroweak scale (left line), respectively.

The scalar potential for  $\rho$ ,  $\eta$  and  $\chi$  is [39, 44]

$$\begin{aligned}
 V(\rho, \eta, \chi) = & \mu_1^2 \eta^\dagger \eta + \lambda_1 (\eta^\dagger \eta)^2 + \mu_2^2 \rho^\dagger \rho \\
 & + \lambda_2 (\rho^\dagger \rho)^2 + \mu_3^2 \chi^\dagger \chi + \lambda_3 (\chi^\dagger \chi)^2 \\
 & + [\lambda_4 (\rho^\dagger \rho) + \lambda_5 (\chi^\dagger \chi)] (\eta^\dagger \eta) \\
 & + \lambda_6 (\rho^\dagger \rho) (\chi^\dagger \chi) + \lambda_7 (\rho^\dagger \eta) (\eta^\dagger \rho) \\
 & + \lambda_8 (\chi^\dagger \eta) (\eta^\dagger \chi) + \lambda_9 (\rho^\dagger \chi) (\chi^\dagger \rho) \\
 & + \frac{1}{2} (f_1 \epsilon^{ijk} \eta_i \rho_j \chi_k + \text{H. c.}).
 \end{aligned} \tag{22}$$

The new gauge bosons acquire masses at several TeV scale when the  $SU(3)_L \times U(1)_Y$  group breaks down to  $SU(2)_L \times U(1)_X$  triggered by the  $SU(3)_L$  scalar triplet  $\chi$ , while the ordinary quarks and SM gauge bosons obtain their masses at the last step symmetry breaking triggered by the triplets  $\eta$  and  $\rho$ . There exist three neutral scalars including the lightest one which corresponds to the SM Higgs boson  $h$  and the other heavier scalar bosons  $H_1^0$  and  $H_2^0$ . By calculating the one-loop effective potential based on Eq.(1) and taking use of the package ‘CosmoTransitions’ [42] in this minimal 3-3-1 model, we find that there are regions of parameters allowed by the collider constraints that can favor a strong first-order phase transition, when the gauge group spontaneously breaks from  $SU(3)_L \times U(1)_Y$  to  $SU(2)_L \times U(1)_X$  as shown in Ref. [39]. During this phase transition, the X field here is just the  $H_1^0$  field. Then, the phase transition GWs spectrum can be obtained from the above GWs spectrum formulae. Since this model has so many free parameters, which makes it very complicated to study the whole parameter regions allowed, we only show one set of benchmark points. For example, when  $v_{\chi_0} = 4$  TeV and  $M_{H_2^0} = 0.8$  TeV, the corresponding GWs spectrum is shown in Fig. 4, which is within the sensitivities of eLISA and BBO.

### C. Phase transition GWs spectrum in other hidden gauge group extended models

In general, if the SM is extended by hidden non-Abelian gauge group, strong first-order phase transition may occur associated with the symmetry breaking at each symmetry breaking scale, where the phase transition GWs may be produced. Then, phase transition GWs can be used to test the hidden gauge symmetry breaking. Besides the above phase transition GWs in the 3-3-1 models, we first discuss the new mechanism, namely, the so called relaxion mechanism [24] proposed in 2015, where the light Higgs mass comes from the dynamical cosmological evolution during the early universe. The relaxion mechanism can technically relax the EW hierarchy [24, 45] and the highest cutoff relaxed in Ref. [24] is about  $10^8$  GeV. The original relaxion mechanism in Ref. [24] need the inflation sector and the QCD-like sector. Especially, one solution to avoid the strong CP problem in the simplest relaxion model, the dark QCD gauge group is needed, where new dark fermions are also included. In some allowed parameter space, the dark

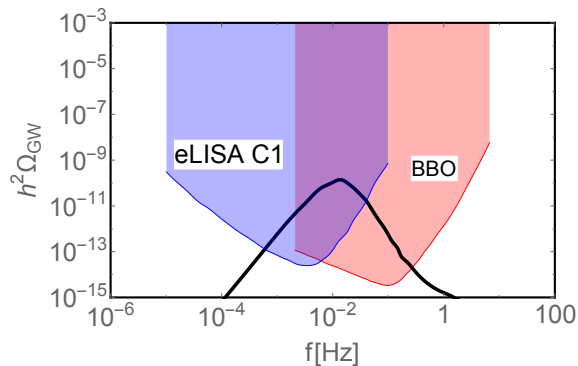


FIG. 4: The GWs spectra  $h^2\Omega_{\text{GW}}$  for the minimal 3-3-1 model. The colored regions correspond to the expected sensitivities of GWs interferometers eLISA and BBO, respectively. The black line depicts the GWs spectrum for the first-order phase transition during  $SU(3)_L \otimes U(1)_Y \Rightarrow SU(2)_L \otimes U(1)_X$  at the TeV scale.

$SU(3)_{\text{dark}}$  can give first-order QCD phase transition at the dark QCD scale. If the dark QCD scale is about  $\mathcal{O}(100)$  MeV, the first-order phase transition can produce phase transition GWs with the peak frequency in the  $10^{-9} - 10^{-7}$  Hz range, which can be probed by the PTA GWs experiments, such as the SKA or FAST<sup>3</sup>. A schematic GWs spectrum for the dark QCD phase transition is shown in Fig. 5. Very recently, a novel mechanism called “ $N$ naturalness” [27] has been proposed to solve the electroweak hierarchy problem by introducing  $N$  copies of the SM with varying values of the Higgs boson mass parameter in a unique universe. Although, the special reheaton particle has been added to the “ $N$ ”naturalness mechanism to suppress the baryogenesis from other copies with  $v \neq 246$  GeV, the first-order phase transition may still happen in some parameter spaces and produce detectable GWs signals, which will be carefully discussed in our future work [46]. However, we show that if a first-order phase transition takes place at a critical temperature of  $\mathcal{O}(10^7 - 10^8)$  GeV [4, 47], such as some versions of grand unified models, this could potentially produce detectable GWs spectrum in the future aLIGO experiments, and provide us with a unique probe of the hidden gauge symmetry breaking at high energy scales.

---

<sup>3</sup> The phase transition GWs signals in dark matter models with  $SU(N)$  hidden gauge group are discussed in [3].



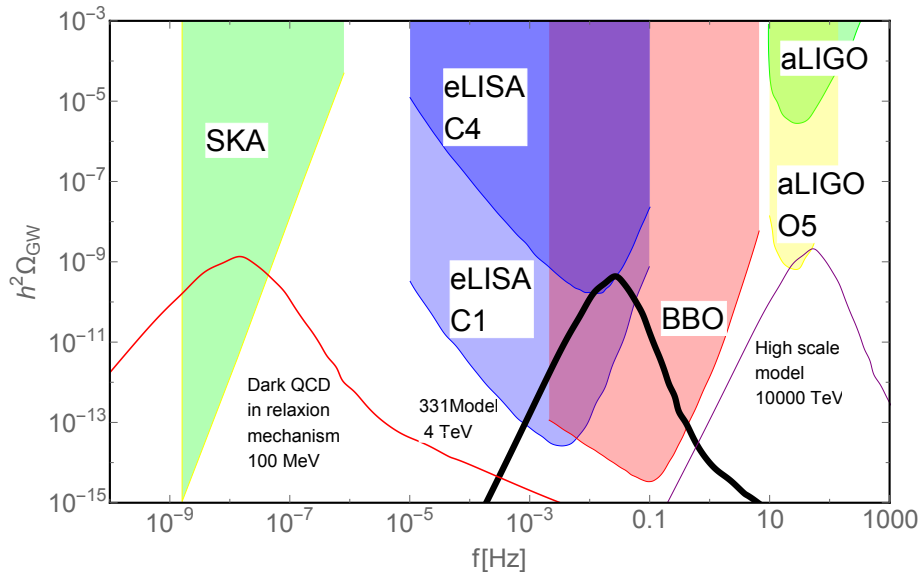


FIG. 5: The phase transition GWs spectra  $h^2\Omega_{\text{GW}}$  from first-order phase transition during the evolution of our universe. The colored regions represent the expected sensitivities of GWs detectors aLIGO, eLISA, BBO and SKA, respectively. The red line depicts the possible GWs spectrum where the first-order phase transition occurs at the energy scale of  $\mathcal{O}(100)$  MeV in some dark QCD models. The black line represents the GWs spectrum for the first-order phase transition at about 4 TeV in some dark gauge group models, such as some 3-3-1 models. The purple line corresponds to the GWs spectrum when the first-order phase transition takes place at the energy scale of  $\mathcal{O}(10000)$  TeV in some models with high symmetry breaking scale.

#### IV. DISCUSSIONS AND CONCLUSIONS

In Fig. 5, the first-order phase transition GWs spectra  $h^2\Omega_{\text{GW}}$  during the evolution of our universe are shown for a generic classes of hidden gauge group extended models at the different energy scales. The colored regions represent the expected sensitivities of GWs detectors SKA, BBO, eLISA and aLIGO, respectively. The red line depicts the possible GWs spectrum where the first-order phase transition occurs at the energy scale of  $\mathcal{O}(100)$  MeV in some dark QCD models. The GWs produced in the dark QCD models can be detected by the PTA experiments, such as the planned SKA or the FAST built in China. The black line represents the GWs spectrum for the first-order phase transition at about 4 TeV in some dark gauge group extended models, such as some versions of 3-3-1 models. We have shown that all the three versions of the 3-3-1 models discussed above could produce strong first-order phase transition GWs at TeV scale when the dark gauge symmetry  $SU(3)_L \otimes U(1)_Y$  breaks to  $SU(2)_L \otimes U(1)_X$ . Especially, in the economical and reduced minimal 3-3-1 models two times first-order phase transition may take place, which will produce two GWs spectra with different characteristic peak frequencies. In general, the phase transition GWs produced at the scale from  $\mathcal{O}(100)$  GeV to several TeV can be tested at future laser interferometer GWs detectors in space, such as the planned eLISA, BBO, Taiji and Tianqin [48]. The purple line corresponds to the GWs spectrum when the first-order phase transition takes place at the energy scale of  $\mathcal{O}(10000)$  TeV in some high scale models, which may be within the sensitivity of the future aLIGO and provide us with a unique detection of the hidden gauge symmetry breaking at high energy scales beyond the abilities of particle colliders. Besides these schematic models, many other hidden gauge group extended models may also undergo one or several times first-order phase transition at different energy scale as shown in Fig.1, where the corresponding phase transition GWs spectra can be produced and tested at the corresponding GWs detectors.

To conclude, phase transition GWs becomes a new and realistic approach to explore the particle cosmology and fundamental physics. From the aspect of cosmology, our universe may undergo one or several times phase transition during the early evolution of the universe. And we can hear the cosmological phase transition using the phase transition GWs if there exists first-order phase transition. From the aspect of particle physics, this phase transition GWs approach can compensate for the collider experiments to explore the hidden gauge group extended models and provide a novel approach to probe the symmetry breaking or phase transition patterns. More detailed study will be discussed in the future.

*Acknowledgements.*

We thank Andrew J. Long, Lian-Tao Wang and Nima Arkani-Hamed for helpful discussions and comments during the workshop on CEPC physics. FPH and XZ are supported in part by the NSFC (Grant Nos. 11121092, 11033005, 11375202) and by the CAS pilotB program. FPH is also supported by the China Postdoctoral Science Foundation under Grant No. 2016M590133.

- 
- [1] B. P. Abbott *et al.* [LIGO Scientific and Virgo Collaborations], Phys. Rev. Lett. **116**, no. 6, 061102 (2016) [arXiv:1602.03837 [gr-qc]].
  - [2] F. P. Huang, Y. Wan, D. G. Wang, Y. F. Cai and X. Zhang, Phys. Rev. D **94**, no. 4, 041702 (2016) doi:10.1103/PhysRevD.94.041702 [arXiv:1601.01640 [hep-ph]].
  - [3] P. Schwaller, Phys. Rev. Lett. **115**, 181101 (2015) [arXiv:1504.07263 [hep-ph]].
  - [4] P. S. B. Dev and A. Mazumdar, Phys. Rev. D **93**, no. 10, 104001 (2016) doi:10.1103/PhysRevD.93.104001 [arXiv:1602.04203 [hep-ph]].
  - [5] J. Jaeckel, V. V. Khoze and M. Spannowsky, Phys. Rev. D **94**, no. 10, 103519 (2016) doi:10.1103/PhysRevD.94.103519 [arXiv:1602.03901 [hep-ph]].
  - [6] H. Yu, B. M. Gu, F. P. Huang, Y. Q. Wang, X. H. Meng and Y. X. Liu, arXiv:1607.03388 [gr-qc].
  - [7] A. Addazi, arXiv:1607.08057 [hep-ph].
  - [8] P. Huang, A. J. Long and L. T. Wang, Phys. Rev. D **94**, no. 7, 075008 (2016) doi:10.1103/PhysRevD.94.075008 [arXiv:1608.06619 [hep-ph]].
  - [9] F. P. Huang and C. S. Li, Phys. Rev. D **92**, no. 7, 075014 (2015) doi:10.1103/PhysRevD.92.075014 [arXiv:1507.08168 [hep-ph]].
  - [10] F. P. Huang, P. H. Gu, P. F. Yin, Z. H. Yu and X. Zhang, Phys. Rev. D **93**, no. 10, 103515 (2016) doi:10.1103/PhysRevD.93.103515 [arXiv:1511.03969 [hep-ph]].
  - [11] V. Vaskonen, arXiv:1611.02073 [hep-ph].
  - [12] E. Witten, Phys. Rev. D **30**, 272 (1984).
  - [13] C. J. Hogan, Phys. Lett. B **133**, 172 (1983); C. J. Hogan, Mon. Not. Roy. Astron. Soc. **218**, 629 (1986).
  - [14] M. S. Turner and F. Wilczek, Phys. Rev. Lett. **65**, 3080 (1990).
  - [15] M. Kamionkowski, A. Kosowsky and M. S. Turner, Phys. Rev. D **49**, 2837 (1994) [astro-ph/9310044].
  - [16] M. Hindmarsh, S. J. Huber, K. Rummukainen and D. J. Weir, Phys. Rev. Lett. **112**, 041301 (2014) [arXiv:1304.2433 [hep-ph]].
  - [17] A. Kosowsky, A. Mack and T. Kahniashvili, Phys. Rev. D **66**, 024030 (2002) [astro-ph/0111483].
  - [18] C. Caprini, R. Durrer and G. Servant, JCAP **0912**, 024 (2009) [arXiv:0909.0622 [astro-ph.CO]].
  - [19] M. Hindmarsh, S. J. Huber, K. Rummukainen and D. J. Weir, Phys. Rev. D **92**, 123009 (2015) [arXiv:1504.03291 [astro-ph.CO]].
  - [20] F. Pisano and V. Pleitez, Phys. Rev. D **46**, 410 (1992) doi:10.1103/PhysRevD.46.410 [hep-ph/9206242].
  - [21] P. H. Frampton, Phys. Rev. Lett. **69**, 2889 (1992). doi:10.1103/PhysRevLett.69.2889
  - [22] P. A. Seoane *et al.* [eLISA Collaboration], arXiv:1305.5720 [astro-ph.CO].
  - [23] V. Corbin and N. J. Cornish, Class. Quant. Grav. **23**, 2435 (2006) [gr-qc/0512039].
  - [24] P. W. Graham, D. E. Kaplan and S. Rajendran, Phys. Rev. Lett. **115**, no. 22, 221801 (2015) doi:10.1103/PhysRevLett.115.221801 [arXiv:1504.07551 [hep-ph]].
  - [25] R. Smits, M. Kramer, B. Stappers, D. R. Lorimer, J. Cordes and A. Faulkner, Astron. Astrophys. **493**, 1161 (2009) doi:10.1051/0004-6361:200810383 [arXiv:0811.0211 [astro-ph]].
  - [26] G. Hobbs, S. Dai, R. N. Manchester, R. M. Shannon, M. Kerr, K. J. Lee and R. Xu, arXiv:1407.0435 [astro-ph.IM].
  - [27] N. Arkani-Hamed, T. Cohen, R. T. D'Agnolo, A. Hook, H. D. Kim and D. Pinner, arXiv:1607.06821 [hep-ph].
  - [28] M. Quiros, hep-ph/9901312.
  - [29] A. D. Linde, Nucl. Phys. B **216**, 421 (1983) Erratum: [Nucl. Phys. B **223**, 544 (1983)]. doi:10.1016/0550-3213(83)90293-6, 10.1016/0550-3213(83)90072-X
  - [30] S. R. Coleman, Phys. Rev. D **15**, 2929 (1977) Erratum: [Phys. Rev. D **16**, 1248 (1977)]. doi:10.1103/PhysRevD.15.2929, 10.1103/PhysRevD.16.1248
  - [31] C. G. Callan, Jr. and S. R. Coleman, Phys. Rev. D **16**, 1762 (1977). doi:10.1103/PhysRevD.16.1762
  - [32] C. Grojean and G. Servant, Phys. Rev. D **75**, 043507 (2007) [hep-ph/0607107];
  - [33] C. Caprini *et al.*, JCAP **1604**, no. 04, 001 (2016) doi:10.1088/1475-7516/2016/04/001 [arXiv:1512.06239 [astro-ph.CO]].
  - [34] J. R. Espinosa, T. Konstandin, J. M. No and G. Servant, JCAP **1006**, 028 (2010) [arXiv:1004.4187 [hep-ph]].
  - [35] P. Binetruy, A. Bohe, C. Caprini and J. F. Dufaux, JCAP **1206**, 027 (2012) [arXiv:1201.0983 [gr-qc]].
  - [36] S. J. Huber and T. Konstandin, JCAP **0809**, 022 (2008) [arXiv:0806.1828 [hep-ph]].
  - [37] R. Jinno and M. Takimoto, Phys. Rev. D **95**, no. 2, 024009 (2017) doi:10.1103/PhysRevD.95.024009 [arXiv:1605.01403 [astro-ph.CO]].
  - [38] Q. H. Cao and D. M. Zhang, arXiv:1611.09337 [hep-ph].
  - [39] J. S. Borges and R. O. Ramos, Eur. Phys. J. C **76**, no. 6, 344 (2016) doi:10.1140/epjc/s10052-016-4168-8 [arXiv:1602.08165 [hep-ph]].
  - [40] V. Q. Phong, H. N. Long, V. T. Van and L. H. Minh, Eur. Phys. J. C **75**, no. 7, 342 (2015) doi:10.1140/epjc/s10052-015-3550-2

- [arXiv:1409.0750 [hep-ph]].
- [41] V. Q. Phong, V. T. Van and H. N. Long, Phys. Rev. D **88**, 096009 (2013) doi:10.1103/PhysRevD.88.096009 [arXiv:1309.0355 [hep-ph]].
  - [42] C. L. Wainwright, Comput. Phys. Commun. **183**, 2006 (2012) doi:10.1016/j.cpc.2012.04.004 [arXiv:1109.4189 [hep-ph]].
  - [43] C. Salazar, R. H. Benavides, W. A. Ponce and E. Rojas, JHEP **1507**, 096 (2015).
  - [44] M. D. Tonasse, Phys. Lett. B **381**, 191 (1996) doi:10.1016/0370-2693(96)00481-9 [hep-ph/9605230].
  - [45] F. P. Huang, Y. Cai, H. Li and X. Zhang, Chin. Phys. C **40**, no. 11, 113103 (2016) doi:10.1088/1674-1137/40/11/113103 [arXiv:1605.03120 [hep-ph]].
  - [46] F. P. Huang, and X. Zhang, work in progress.
  - [47] C. Balazs, A. Fowlie, A. Mazumdar and G. White, arXiv:1611.01617 [hep-ph].
  - [48] J. Luo *et al.* [TianQin Collaboration], Class. Quant. Grav. **33**, no. 3, 035010 (2016) doi:10.1088/0264-9381/33/3/035010 [arXiv:1512.02076 [astro-ph.IM]].